Journal of Molecular and Cellular Cardiology 132 (2019) 71–83

Contents lists available at ScienceDirect

Journal of Molecular and Cellular Cardiology

journal homepage: www.elsevier.com/locate/yjmcc

Novel mediators of aneurysm progression in bicuspid aortic valve disease

Stephanie W. Tobin[a], Faisal J. Alibhai[a], Myunghyun M. Lee[a,c], Azadeh Yeganeh[a], Jie Wu[a,b], Shu-Hong Li[a], Jian Guo[a], Katherine Tsang[a,c], Laura Tumiati[a,c], Rodolfo Rocha[a,c], Jagdish Butany[d], Terrence M. Yau[a,c], Maral Ouzounian[a,c], Tirone E. David[a,c], Richard D. Weisel[a,c], Ren-Ke Li[a,c,*]

[a] Division of Cardiovascular Surgery, Toronto General Hospital Research Institute and Peter Munk Cardiac Centre, University Health Network, Toronto, ON, Canada
[b] Laboratory of Medical Genetics, Harbin Medical University, Harbin, China
[c] Department of Surgery, Division of Cardiac Surgery, University of Toronto, Toronto, ON, Canada
[d] Department of Pathology, University Health Network, Toronto, ON, Canada

ARTICLE INFO

Keywords:
Bicuspid aortic valve
Aneurysm
AP-1

ABSTRACT

Bicuspid aortic valve (BAV) disease is a congenital abnormality that is associated with ascending aortic aneurysm yet many of the molecular mechanisms remain unknown. To identify novel molecular mechanisms of aneurysm formation we completed microarray analysis of the proximal (severely dilated) and distal (less dilated) regions of the ascending aorta from five patients with BAV. We identified 180 differentially expressed genes, 40 of which were validated by RT-qPCR. Most genes had roles in inflammation and endothelial cell function including cytokines and growth factors, cell surface receptors and the Activator Protein 1 (AP-1) transcription factor family (*FOS, FOSB* and *JUN*) which was chosen for further study. AP-1 was differentially expressed within paired BAV aneurysmal samples ($n = 8$) but not Marfan patients ($n = 5$). FOS protein was significantly enriched in BAV aortas compared to normal aortas but unexpectedly, ERK1/2 activity, an upstream regulator of FOS was reduced. ERK1/2 activity was restored when BAV smooth muscle cells were cultured in vitro. An mRNA-miRNA network within paired patient samples identified AP-1 as a central hub of miRNA regulation. FOS knockdown in BAV SMCs increased expression of miR-27a, a stretch responsive miRNA. AP-1 and miR-27a were also dysregulated in a mouse model of aortic constriction. In summary, this study identified a central role for AP-1 signaling in BAV aortic dilatation by using paired mRNA-miRNA patient sample. Upstream analysis of AP-1 regulation showed that the ERK1/2 signaling pathway is dysregulated and thus represents a novel chain of mediators of aortic dilatation in BAV which should be considered in future studies.

1. Introduction

Bicuspid aortic valve (BAV) disease is a congenital abnormality present in 1–2% of the population in which the aortic valve is composed of two functional leaflets instead of three [1]. Several complications may develop in the valve because of this birth defect including stenosis and regurgitation. Those born with BAV are also prone to aortic expansion [2] which can lead to aortic dissection or rupture but the cause of these complications are unclear. Thus, understanding the mechanisms responsible for aortic dilatation is important to develop a treatment strategy. To prevent further aortic expansion and these complications, patients may have the ascending aorta excised and replaced with a Dacron tube graft [1]. Patients with BAV may have the valve preserved or replaced at the same time as their aortic surgery [3].

Aortic aneurysm in BAV may result from a combination of altered blood flow velocity or unidentified genetic abnormalities, and dilatation worsens with age [3]. Even without stenosis, BAV changes blood flow direction and velocity profile in the ascending aorta, leading many to believe hemodynamics may be a major participating factor contributing to aneurysm formation [3]. Several genetic components have also been implicated in BAV but none have been shown to be causative in aortic dilatation. For example, degradation of the extracellular matrix (ECM) is enhanced in BAV due to an upregulation in the activity of matrix metallopeptidases (MMPs) and downregulation of tissue inhibitors of metalloproteinases (TIMPs) [4]. This unbalanced TIMP: MMP ratio is also seen in Marfan syndrome, an inheritable disease of the connective tissue caused by a mutation in Fibrillin-1 [5]. Patients with Marfan syndrome are also likely to develop aortic aneurysm, but

Abbreviations: BAV, Bicuspid Aortic Valve; TAV, Tricuspid Aortic Valve; AP-1, Activator Protein 1; TGF-β, Transforming Growth Factor β; ERK1/2, Extracellular signal related kinase 1/2; MMP, Matrix Metallopeptidase; ECM, Extracellular Matrix; TIMP, Tissue Inhibitor of Metalloprotease

* Corresponding author at: Princess Margaret Cancer Research Tower, Room 3-702, 101 College St., Toronto, ON M5G 1L7, Canada.
E-mail address: renkeli@uhnres.utoronto.ca (Ren-Ke Li).

https://doi.org/10.1016/j.yjmcc.2019.04.022
Received 21 December 2018; Received in revised form 6 April 2019; Accepted 20 April 2019
Available online 29 April 2019
0022-2828/

the molecular changes have been more clearly described. Loss of Fibrillin-1 releases TGF-β in the extracellular space which mediates downstream transcriptional changes of matrix remodelling programs including increased MMP activity [5]. TGF-β has also been implicated in BAV aneurysm progression but its role is controversial. While some groups have found increased expression of TGF-β in BAV aneurysmal tissue [6,7], others have documented the opposite trend and argue that TGF-β signaling may be impaired [8,9].

As aortic aneurysm in BAV patients is progressive, a comparison of aneurysmal tissue from the proximal (severely dilated) and distal (less dilated) regions within the same patient could provide insight into the molecular changes that drive this disease. Using this strategy we have previously identified that miR-17 expression is higher in the less dilated region of the diseased aorta of BAV patients [4]. miR-17 can repress TIMP-1 translation, thereby promoting MMP activity and aortic dilatation. Intervention to prevent the progressive development of aortic dilatation could reduce the need for additional surgery beyond the ascending aorta, but there is still much unknown about the molecular changes that initiate remodelling. To this end, we completed microarray analysis of the dilated ascending aorta from five patients with BAV and characterized molecular changes.

2. Methods

2.1. Patient information and tissue collection

This study was approved by the Research Ethics Board of the University Health Network and complies with the Declaration of Helsinki. Aortic specimens were collected after patients provided informed written consent. Samples from severely dilated and less dilated sections of ascending aortas from 15 BAV patients, 5 Marfan patients, 5 TAV patients and 5 normal aorta samples (TAV; non-aneurysmal). The ascending aorta of the patients with aortic aneurysm has been described previously [4]. The tissue was divided into the proximal and distal regions to identify new pathways involved in aortic tissue remodelling. Control aortic tissue specimens were collected using a 5 mm aortic punch employed for the proximal anastomosis during coronary artery bypass graft surgery from control patients with normal-appearing ascending aortas. All aortic samples were quickly frozen in liquid nitrogen and stored at −80 °C for RNA or protein studies. In addition, fresh aortic segments were placed in Dulbecco's Modified Eagle Medium with 10% fetal bovine serum (Life Technologies) for isolation of smooth muscle cells (SMCs). RNA and protein analysis are detailed below.

2.2. Microarray analysis

Five sets of paired proximal-distal BAV samples were used in microarray analysis. RNA samples were labelled using Illumina TotalPrep-96 RNA Amplification kit (Ambion). Complimentary RNA generated from these samples were hybridized onto one Human HT-12 V4 BeadChip and incubated at 58 °C with rotation speed 5 for 18 h for hybridization. The BeadChip was washed and stained as per Illumina protocol and scanned on the iScan (Illumina). Data were quantified in GenomeStudio Version 2011.1 (Illumina).

Data were loaded into GeneSpring v12.6 for analysis. Data were normalized using a standard quantile normalization followed by a “per probe” median centred normalization. Probes with no signal were removed. Only probes that were above the 20th percentile of the distribution of intensities in 80% of the groups were allowed to pass through this filtering. Differentially expressed genes were identified using a paired, two tailed *t*-test ($p < .05$) that had a fold change greater than ± 1.2. R statistical computing software was used to generate clustering heatmaps and volcano plots. Gene Ontology Biological Processes were identified using DAVID. Transcription factor binding sites were identified using oPossum3.0. Cytoscape v3.4 was used to visualize the AP-1 target gene network.

2.3. RT-qPCR analysis

Tissue was homogenized into a fine powder over liquid nitrogen. RNA was extracted using TriReagent (Sigma-Aldrich). cDNA was prepared from 1 μg of total RNA using Lucigen Reverse Transcriptase. Equal amount of cDNA was combined with SybrGreen (SensiFAST SybrGreen HiRox, BioLine) or Taqman reagent (Taqman Universal PCR Master Mix, no AmpErase UNG, ThermoFisher) according to the manufacturer's recommendations. SybrGreen was run using the following parameters: 95 °C (2 min) followed by [95 °C 5 s, 60 °C, 30 s] × 40 cycles. For Taqman analysis, samples were heated to 95 °C for 10 min followed by [95 °C for 15 s, 60 °C for 1 min] × 40 cycles. Data were normalized to *β-Actin* or *Gapdh* using the delta-delta Ct method. Expression of human *TIMP1, PDGFD, MMP-2, MMP-9, CCN2, DUSP1* and *DUSP6* and all mouse cDNA was analyzed using SybrGreen while all others were analyzed by Taqman. Primer sequences are available upon request. Genes were identified to have a strong role in inflammation/immune cell function or angiogenesis/endothelial cell function if they were annotated under a related gene ontology term or a moderate role if they were identified in relevant publications.

2.4. Western blot analysis

Tissue was homogenized into a fine powder over liquid nitrogen. Protein was extracted via sonication (10s pulses × 4) in lysis buffer (50 mM Tris (pH 8.0), 150 mM NaCl, 1% NP-40, 1 mM β-glycerolphosphate, 1 mM Na_3VO_4, 1 μg/mL leupeptin, 1 μg/mL pepstatin, 1 mM phenylmethylsulfonyl fluoride, Sigma-Aldrich). Total protein (40 μg) was loaded into a 10% polyacrymlamide gel. Protein was transferred onto nitrocellulose at 100 V for 1 h. Membranes were blocked using 5% milk in TBS-T (0.1%) for 1–2 h at room temperature. Primary antibodies were incubated overnight at 4 °C with rocking. Secondary antibodies were incubated for 1–2 h at room temperature. Protein bands were visualized using chemiluminescence (GE Healthcare). The following antibodies were used in western blot: c-Jun (sc-1694, 1:100), c-FOS (sc-52, 1:100), ERK1/2 (Cell Signaling 9102, 1:500), p-ERK1/2 (Cell Signaling 9106, 1:250), GAPDH (Millipore MAB374, 1:2000), Goat anti-Rabbit (sc-2030, 1:2000), Goat anti-mouse (sc-2005, 1:2000). Protein expression was assessed using ImageJ.

2.5. Immunofluorescence

Four patients with BAV were assessed by immunofluorescence. Samples were fixed in 2% PFA and then embedded in OCT. Aortic segments were cut into 5 μm sections. Cultured SMCs and sectioned tissue were treated as follows: Samples were treated with 0.2% Triton-X for membrane permeabilization for 5 min. Blocking buffer (5% Goat Serum) was added for 15 min. The slides were incubated with primary antibodies FOS (Sigma HPA018531, 1:50), CD45 (BD, 555480, 1:100), pFOSThr325 (Thermo-Fisher, 44-281G, 1:100), MMP-2 (Abcam, 1:100 ab27150) or Smooth Muscle Actin (Sigma, A-2547, 1:400) in 1.5% Goat Serum for 1–2 h at room temperature. Incubation with secondary antibodies was carried out at room temperature with light protection for 1 h. The secondary antibodies used were Donkey anti-Rabbit Alexa546 (ThermoFisher A-10040) and Donkey anti-Mouse Alexa647 (ThermoFisher A-31571) both at 1:400. The nuclei were identified with 4′,6-diamidino-2-phenylindole (DAPI, Sigma). FOS and SMA images were captured using an Olympus CM10 microscope (Olympus Canada). The FOS and SMA signals were digitally recoloured to green and red, respectively. Three patient aortic sections were used for quantification of CD45. The number of $CD45^+$ cells per patient were averaged from three regions of interest. CD45 images were captures using a Zeiss LSM700 confocal microscope, and the digital images were processed with Zeiss ZEN. Cultured SMCs were imaged using the Nikon Eclipse Ti–S.

2.6. Human aortic SMC isolation and culture

Smooth muscle cells from patients with BAV were isolated as previously described [4]. Briefly, human aortic smooth muscle cells were cultured in Medium 231, with 5% Smooth Muscle Growth Supplement, 100 U/mL penicillin G, and 100 μg/mL streptomycin (Life Technologies) in a humidified incubator at 37 °C with 5% CO_2, during passages 2–4. Cells were placed in serum-free DMEM (ThermoFisher) overnight (16 h). The next day, serum-free medium supplemented with TGF-β (Preprotech, 100-21) was added to cells for 4 h (10 ng/mL). After TGF-β treatment, protein was collected for western blot analysis. For AP-1 inhibition, SR 11302 (Cayman, 16,338) was added to normal culture medium for 24 h at10 μM, after which, RNA was collected and processed as described. For siRNA experiments, cells were transfected at 90% confluence using 50 nM of siFOS (Sigma, SASI_Hs01_00184572) or scrambled control (Qiagen AllStars Negative Control, SI03650318) using Lipofectamine 2000 (ThermoFisher), as per the manufacturer's recommendations. RNA was isolated 48 h post-transfection.

2.7. Supravalvular aortic constriction

The Animal Care Committee of the University Health Network approved all experimental procedures which were carried out according to the Guide for the Care and Use of Laboratory Animals (NIH, revised 2011). Female C57BL/6 mice weighing 30 g were used for these experiments. Anesthesia was induced with 5% isoflurane after which animals were intubated and maintained at 2% isoflurane for the duration of the procedure. Following a midline skin incision, the animal underwent a superior median hemisternotomy. A sternal retractor was used to visualize the intrathoracic cavity. Thymic fat was resected and the ascending aorta was isolated circumferentially from its surrounding connective tissues using blunt and sharp dissection. A 7-0 silk tie was positioned along the posterior aspect of the ascending aorta through the transverse sinus. A 20-gauge needle was placed along the anterior aspect of the ascending aorta. Two slipknots and a securing knot were used to tie the needle and the ascending aorta together. The needle was removed and the suture tails were trimmed at 0.5 cm. Valsalva maneuver was used to inflate the lungs. Animals were closed, iodine applied over the incision, and buprenorphine given for analgesia (0.05 mg/kg, s.c.). Animals were weaned from the ventilator and placed in a warmed cage for further recovery.

2.8. Echocardiography

Echocardiography was performed at baseline prior to aortic constriction. Following constriction, the animals underwent echocardiography to confirm hemodynamic changes as measured by an increase in the maximum systolic flow velocity and derived pressure gradient in the ascending aorta. Animals were monitored weekly for up to 4 weeks after constriction. Primary endpoints comprised of the maximum flow velocities, derived pressure gradients, and diameters in the ascending aorta. The thoracic aorta including the ascending, arch, and descending segments were visualized on each echocardiography for all animals. Ascending aortic diameters were measured proximal to the origin of the innominate artery orthogonally to the long-axis of the ascending aorta. This anatomical landmark was used throughout the study to maintain consistency in the location of aortic measurements in subsequent echocardiographic analyses. Secondary endpoints consisted of left ventricular ejection fraction, end-diastolic and end-systolic dimensions, and fractional shortening (Supplementary Table 2).

2.9. miRNA profiling and bioinformatics analysis

MicroRNA expression was assessed using the Nanostring platform (Nanostring Technologies) using previously published miRNA data from BAV patient samples [4]. Raw counts were normalized to positive controls and top 100 expression reads. Negative controls were used to set the background threshold. Differential expression of 800 miRNAs were screened in 5 paired distal and proximal patient samples. MicroRNAs exhibiting ≥2.0-fold change and $p < .05$ were included for further analysis. Predicted target mRNAs of differentially expression miRNAs was determined using miRDIP (http://ophid.utoronto.ca/mirDIP/) [10]. Only targets present within 5 databases were considered, and for increased stringency the top two-thirds of targets were chosen. Predicted target mRNAs were then compared to differentially expressed mRNAs (≥1.5 f.c., $p < .05$) identified between distal and proximal aorta samples in order to determine which differentially expressed miRNAs target differentially expressed mRNAs. This list of miRNAs which target differentially expressed mRNAs was used for all further analyses. Predicted transcription factors of differentially expressed miRNAs was determined using TransmiR v2.0 (http://www.cuilab.cn/transmir) [11]. Using predicted miRNA transcription factors, miRNA-mRNA pairs, mRNA log2 expression, and miRNA log2 expression, a network of miRNA-mRNA interaction was built using Cytoscape v3.7.1. Linear regression analysis of miRNA-mRNA expression was assessed using BioVinci (BioTuring).

In order to compare previously identified smooth muscle stretch responsive genes with differentially expressed genes identified in our samples, publicly accessible data deposited in Gene Expression Omnibus was analyzed using GEO2R; GSE1595 [12], GSE21663 [13], and GSE47687 [14]. As the number of studies investigating smooth muscle stretch with deposited data were limited, the search was extended to include studies profiling stretch dependent changes in aortic valves cusp and interstitial cells. Predicted transcription factors of stretch responsive genes was determined using OPOSSUM v3.0 (http://opossum.cisreg.ca/).

2.9.1. Gene set enrichment map

Gene enrichment map analysis was performed as described previously [15]. First, differentially expressed genes were analyzed using gene set enrichment analysis (GSEA) to determine significantly enriched gene ontology terms [16]. GSEA terms were clustered using Cytoscape v.3.7.1 and the Enrichment Map plugin. Nodes represent gene sets and edges represent overlap scores which are determined by the number of genes-sets shared by nodes. Generic gene-sets (e.g. Protein Complex Assembly) were manually removed to optimize the map layout. Similar nodes are arranged so that nodes of similar gene sets are clustered together.

2.9.2. miRNA profiling

Total RNA was isolated using Tri-reagent (Sigma) for tissue or miRNeasy (Qiagen) for cells. 40 ng of RNA was reverse transcribed using the miRCURY LNA RT Kit (Qiagen) according to the manufacturer's instructions. MicroRNA expression was assessed using SYBR green and LNA primers (Qiagen) to *hsa-miR-181a-5p, hsa-miR-27a-3p, hsa-miR-144-5p, hsa-miR-199a-5p, hsa-miR-451a* and *hsa-miR-103a-3p*. *miR-103a-3p* was used as a loading control, as U6 expression substantially different between samples.

2.10. Statistical Analysis

All values are expressed as mean ± SEM. When only samples of proximal and distal BAV samples were compared a paired two tailed *t*-test was performed. If three or more samples were compared a one-way ANOVA was performed followed by Tukey's post-hoc analysis.

3. Results

3.1. Identification of differentially expressed genes in diseased BAV tissue

The Proximal (severely dilated) and Distal (less dilated) regions of dilated aortas from five patients with BAV were collected and prepared

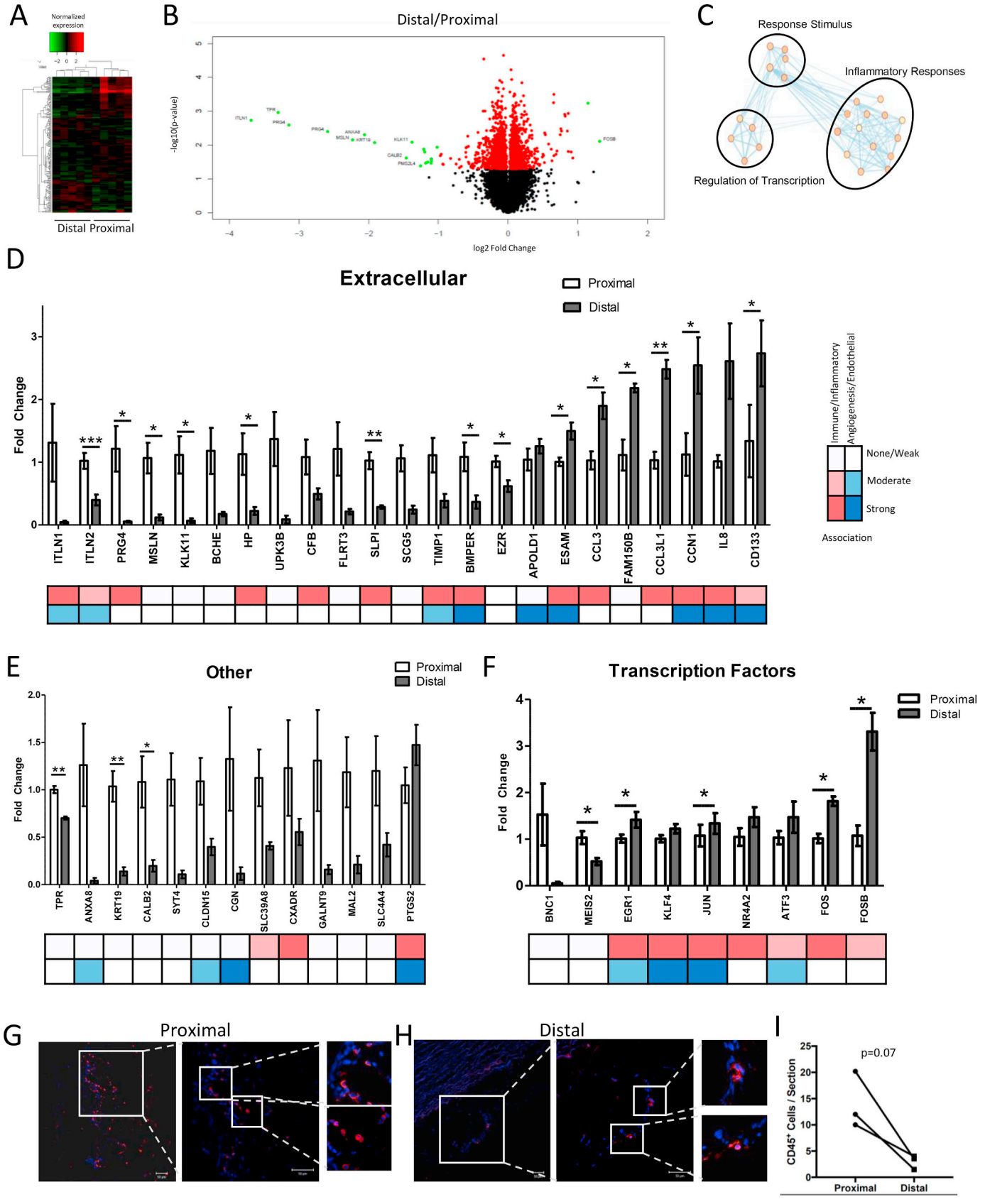

(caption on next page)

Fig. 1. Differential activation of inflammatory and endothelial signaling pathways in BAV aneurysmal aortic tissue. A) Heat map depicting hierarchical clustering of 195 differentially expressed gene probes in the proximal and distal aorta from BAV patients ($n = 5$, $p < .05$, FC $> \pm 1.2$). B) Volcano plot depicting the most up and downregulated genes based on the ratio of expression in the Distal/Proximal region. Black: $p > .05$; Red: $p < .05$; Green: $p < .05$ and logFC $> \pm 1.0$. C) Gene set enrichment map of ontology terms. Nodes represent gene sets and edges represent overlap scores which are determined by the number of genes-sets shared by nodes. Similar nodes are arranged so that nodes of similar gene sets are clustered together. D–F) RT-qPCR validation of Extracellular factors (D), "Other" gene products with roles in various processes (E) or Transcriptional Regulators (F) ($n = 4$, $^{*}p < .05$, $^{**}p < .01$, $^{***}p < .001$). Ct values were normalized to *β-Actin*. Data were normalized to gene expression in the proximal region of aneurysmal aortic tissue and analyzed using a paired *t*-test. G-H) $CD45^+$ cells (red) are present in the adventitia-media of proximal (G) and distal (H) BAV aneurysmal aorta. I) The number of $CD45^+$ cells in the proximal and distal BAV aorta was quantified in three paired sets. No significant difference in $CD45^+$ cells was detected (paired t-test). (For interpretation of the references to colour in this figure legend, the reader is referred to the web version of this article.)

for microarray analysis. This strategy has been used to identify a role for miR-17 in early tissue remodelling of BAV aortas [4]. A total of 195 differentially expressed probes were identified, representing 180 unique genes (Supplementary Dataset). Fig. 1A depicts the resultant probes in a heatmap using hierarchical clustering and demonstrates a distinction between the gene expression profiles of the Distal and Proximal regions of aorta from BAV patients. The log2 Fold Change in gene expression between the Distal and Proximal regions was mapped using a volcano plot to identify the most differentially expressed probes (Fig. 1B). *FOSB*, a member of the Activator Protein-1 (AP-1) transcription factor family was the most upregulated gene. Several secreted and extracellular factors that have been identified as prognostic markers of disease by others were significantly downregulated in the distal aorta compared to the proximally dilated area such as *ITLN1* (Intelectin 1), *PRG4* (proteoglycan 4), *MSLN* (Mesothelin), and *BCHE* (Butyrylcholinesterase) [17–19].

We next assessed the Biological Processes (BP) that were enriched in our microarray analysis (Supplementary Fig. S1A). The most enriched BP term was "Positive regulation of the ERK1 and ERK2 cascade". Nine of the ten remaining BP terms were involved in cellular responses related to inflammation. As GO terms are subject to redundancy, we also visualized GSEA terms using an enrichment map to better define the processes that differentially expressed genes belong to (Fig. 1C). Clustering of similar GSEA terms revealed 3 distinct biological processes, inflammation, response to stimuli, and transcriptional regulation.

The expression pattern of genes identified by microarray that showed the most dynamic changes in gene expression were validated using RT-qPCR (Fig. 1D–F). *CCN1* and *CD133* expression was assessed as although their expression was not statistically significant they showed high fold change from the array analysis. We generated three broad clusters for analysis: "Extracellular" (Fig. 1D), "Other" (Fig. 1E) and "Transcription" (Fig. 1F) and further classified these genes based on their involvement in inflammation/immune cell function or angiogenesis/endothelial cell function. These data are represented as cumulative group means in Fig. 1 but are also shown as patient pairs in Supplementary Figs. S2–4 which demonstrate gene expression trends more clearly. Putative prognostic markers such as *MSLN, PRG4, TIMP-1* were reduced in the distal aorta compared to the proximal region (Fig. 1D). Conversely inflammation-associated genes *CCL3, CCL3L1, IL8* and *ESAM* (endothelial cell adhesion molecule) were upregulated in the distal aorta. Factors categorized as "Other" included genes that function in calcium signaling (*CALB, SYT4*) and epithelial-related genes (*KRT19, MAL2, EZR* and *CLDN15*) (Fig. 1E).

Genes within the "Transcription" cluster included three members of the AP-1 transcription factor family, *JUN, FOS,* and *FOSB*, AP-1 co-factor *ATF3*, and *NR4A2, KLF4, EGR1, MEIS1,* and *BNC1*. *JUN, FOS* and *FOSB* were significantly upregulated in the distal ascending aorta (Fig. 1F). *JUNB* was also upregulated distally based on the microarray analysis (Supplementary Dataset). In silico predictive modelling was used to determine whether the genes identified in our microarray screen could be regulated by AP-1. Of all differentially expressed genes, 129 contain putative AP-1 consensus sequences (TGACTCA) within 5 kb of the transcription start site (Supplementary Fig. S1B). Potential AP-1 target genes that function in the extracellular space are shown in a schematic in Supplementary Fig. S1C. Upregulated genes are in red, while downregulated genes are in green. This comprehensive bioinformatic analysis identifies AP-1 as a potential driving force in aortic aneurysm in BAV.

To determine whether changes in gene expression patterns were related to regional differences in immune cell recruitment we stained for $CD45^+$ cells in the proximal and distal aortic segments (Fig. 1G–H). $CD45^+$ cells were detected throughout the aneurysmal aorta in the adventitia but there tended to be fewer $CD45^+$ cells present in the distal region (Fig. 1I). This suggests that the upregulation of inflammatory-related genes in the distal aortic segment may be caused by different immune cell subtype activity or the inflammatory signals may be derived from aortic cells such as smooth muscle.

3.2. Expression of Fosb, Fos, Atf3 and Jun in aortic disease

AP-1 can complex as a JUN-JUN, JUN-FOS or JUN-ATF dimer. We hypothesized that upregulation of *FOSB, FOS, ATF3* and *JUN* indicated an important role for AP-1 complexes in aortic disease progression in other aneurysmal tissue in addition to BAV. To test this, we compared the expression of these factors from patients with BAV to normal aortic tissue (Fig. 2A), dilated aorta from patients with Marfan syndrome or phenotypically normal tricuspid aortic valves (TAV; data not shown) with aortic aneurysm in both the distal and proximal regions. Clinical data for each patient are in Supplementary Table 1. Expression of AP-1 factors in aneurysmal TAV samples demonstrated considerable variability and were excluded from this study (data not shown). We evaluated expression *FOSB, FOS, ATF3* and *JUN* in the proximal and distal regions of aortic tissue across all disease states using RT-qPCR (Fig. 2A). Interestingly, while the distal and proximal regions of dilated BAV aorta showed differential expression of *FOSB, FOS, ATF3* and *JUN*, we did not observe differences within Marfan aortic tissue. One patient with both BAV and Marfan (datapoints are blue in the BAV group) showed comparable AP-1 expression trends to BAV samples. When compared to normal aortic tissue, *JUN* was significantly upregulated in distal BAV aortic tissue and *FOS* followed a similar trend. Expression of AP-1 factors in Marfan aneurysmal tissue was not significantly different from normal aorta.

3.3. AP-1 protein and upstream MAPK, ERK1/2, are differentially regulated in BAV aneurysmal tissue

We next assessed changes in AP-1 protein levels in BAV aneurysmal tissue. We focused on JUN and FOS since they compose the classical AP-1 heterodimer. JUN is also the only required AP-1 subunit as it can form homodimers with other JUN family members while the FOS family cannot. Western blot analysis shows that several bands were detected by the FOS and JUN antibodies, potentially representing post-translational modification or degradation (Fig. 2B). In addition to the JUN protein band observed at the predicted molecular weight of 36 kDa, we observed an additional isoform at approximately 25 kDa but only in aneurysmal BAV tissue and not in normal aortic samples. We did not, however, detect a difference in FOS or JUN protein expression between Proximal and Distal samples but compared to normal aortic tissue, FOS protein was strongly upregulated (Fig. 2B).

Next, we examined FOS expression in distal BAV aneurysmal aorta.

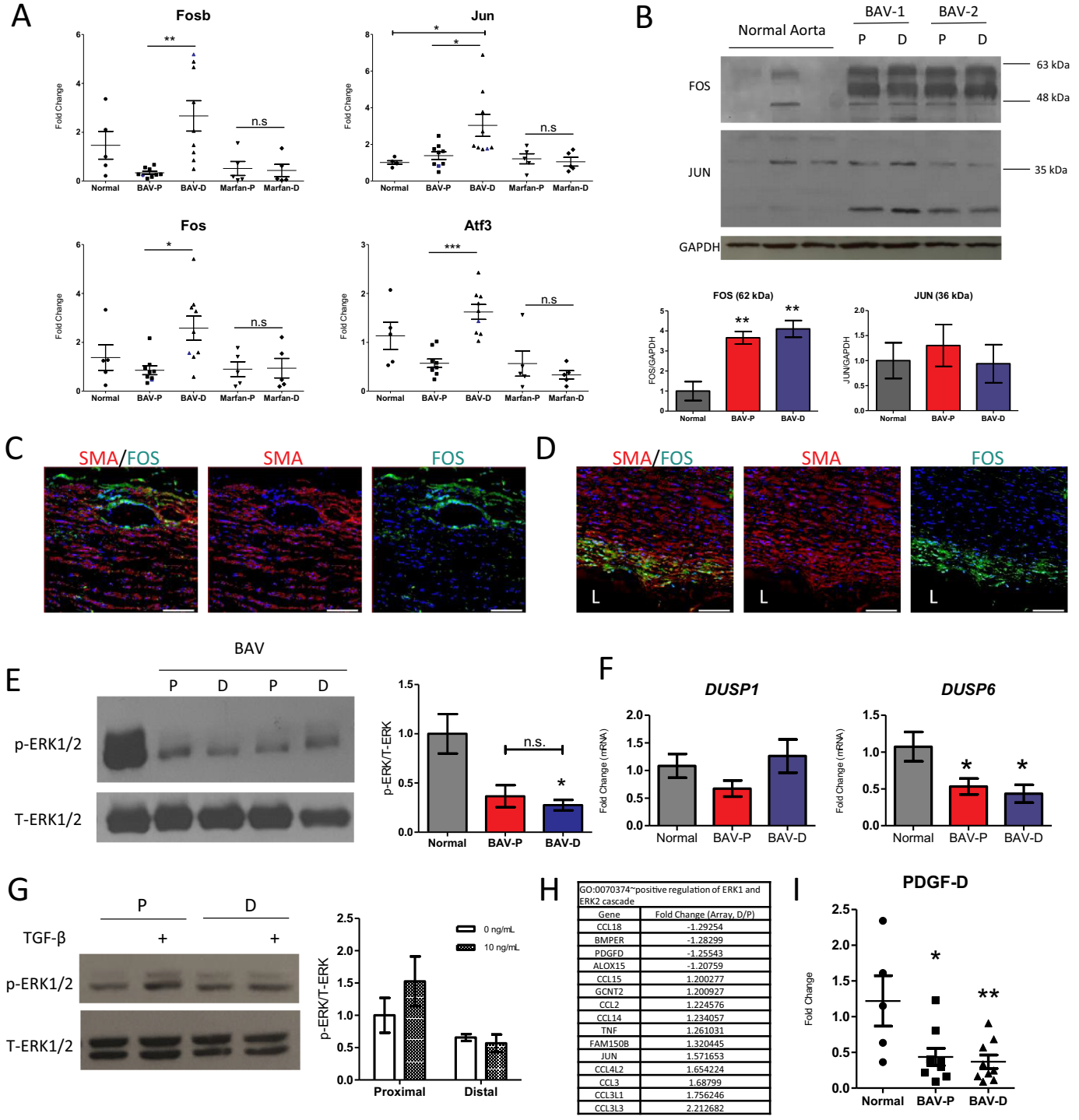

GO:0070374~positive regulation of ERK1 and ERK2 cascade	
Gene	Fold Change (Array, D/P)
CCL18	-1.29254
BMPER	-1.28299
PDGFD	-1.25543
ALOX15	-1.20759
CCL15	1.200277
GCNT2	1.200927
CCL2	1.224576
CCL14	1.234057
TNF	1.261031
FAM150B	1.320445
JUN	1.571653
CCL4L2	1.654224
CCL3	1.68799
CCL3L1	1.756246
CCL3L3	2.212682

Fig. 2. Assessment of AP-1 expression and upstream MAPK activity in dilated aortic tissue shows MAPK-AP-1 pathway uncoupling.
A) Distal (D) and Proximal (P) portions of aortic tissue from BAV or Marfan patients were separated for RT-qPCR analysis of *FOSB, FOS, JUN* and *ATF3* compared to normal aortic tissue. Normal aorta n = 5; BAV $n = 8$; Marfan n = 5; BAV + Marfan ($n = 1$), denoted in blue in the BAV group. Ct values were normalized to *Gapdh*. Data are expressed as the relative fold change to normal aortic tissue (mean ± SEM). $*p < .05$, $**p < .01$ and $***p < .001$ represent statistical significance using a one-way ANOVA. B) FOS expression is increased in BAV aneurysmal aortic tissue. Normal aortic tissue ($n = 3$) and BAV aortic tissue (n = 4) were analyzed via western blot for FOS and JUN expression. Protein expression was normalized to GAPDH. An additional isoform of JUN (~25 kDa) was detected in BAV tissue. Data were analyzed using a one-way ANOVA. C) FOS protein localization in the distal aneurysmal aorta of BAV patients. FOS (green) and Smooth Muscle Actin (SMA, red) was assessed in the adventitia-medial (C) or the endothelial-medial (D) regions. L = lumen. DAPI is depicted in blue. Scale = 100 μm. E) ERK1/2 activity is reduced in BAV aortic tissue. The aneurysmal tissue was divided into Proximal and Distal sections and analyzed by western blot with the respective antibodies. P-ERK1/2 activity was normalized to Total ERK1/2 (T-ERK). Normal aorta n = 4; BAV aorta $n = 3$. $*p < .05$ based on one-way ANOVA. Expression of *DUSP1* (F) and *DUSP6* (G) was assessed using RT-qPCR in BAV (n = 8) and normal aortic tissue (n = 5). G) Smooth muscle cells isolated from the proximal and distal regions in patients with BAV were treated with TGF-β (10 ng/mL) for 4 h in culture before protein analysis. P-ERK1/2 activity was normalized to T-ERK. H) A list of differentially expressed genes, and corresponding fold change values, identified from array analysis as part of the GO term "positive regulation of ERK1 and ERK2 cascade". I) *PDGFD* is reduced in BAV aortic tissue (n = 8) compared to normal aorta (n = 5). Data were analyzed as described above. (For interpretation of the references to colour in this figure legend, the reader is referred to the web version of this article.)

Fig. 2C and D represent the adventitial and intimal regions of the aortic tissue, respectively which were co-stained for smooth muscle actin (SMA) in red. FOS protein (green) was localized to the peripheral regions of the ascending aorta (Fig. 2C). In the adventitia/medial border FOS was detected near blood vessels and SMA negative cells while in the intima/medial border FOS was expressed in SMA positive cells (Fig. 2D).

It is well known that ERK1/2 is a potent regulator of FOS, an immediate early gene, at the transcriptional and post-translational levels [20,21] therefore we assessed ERK1/2 activity in aortic lysates. Surprisingly, ERK1/2 activity was markedly downregulated in BAV aneurysmal tissue. To further understand this finding, we assessed *DUSP1* and *DUSP6* MAPK phosphatase expression. There was no significant change in *DUSP1* expression between BAV and normal aortic tissue (Fig. 2F). *DUSP6* expression however was reduced in both Proximal and Distal BAV aorta sections compared to normal aorta (Fig. 2F). This is particularly striking because ERK1/2 is able to regulate *DUSP6* transcription via a negative feedback loop [22,23]. Downregulation of *DUSP6* corroborates a reduction of ERK1/2 activity in BAV samples. Isolation of SMCs from BAV patients showed that ERK1/2 activity is restored in vitro (Fig. 2G) and may point to environmental regulation such as altered flow or shear stress. Indeed, several genes identified in our study were also enriched in stretch-responsive gene analyses (Supplementary Fig. S5). We attempted to activate the ERK1/2 pathway via TGFβ treatment, however this effect was not robust (Fig. 2G). As the most enriched Biological Processes term was related to the ERK1/2 signaling cascade (Supplementary Fig. S1A) we assessed whether any genes in this list may affect ERK1/2 activity (Fig. 2H). We noticed regional differences in *PDGFD* expression, which has been linked to abdominal aortic aneurysm development [24,25]. Interestingly, compared to normal aortic tissue, *PDGFD* is downregulated in both regions of the BAV aorta, representing a potential mediator of reduced ERK1/2 activity (Fig. 2I).

3.4. AP-1 is associated with a mRNA-miRNA regulatory network

To better understand transcriptional changes which underlie changes in AP-1 expression we examined miRNA expression in the same paired patient samples in which our mRNA array was derived [4]. Based on bioinformatics analysis detailed in Fig. 3A, we identified 27 differentially expressed miRNAs that were predicted to interact with 20 genes from our mRNA array. This unbiased approach revealed that *FOSB, FOS, ATF3* and *JUN* are a part of this miRNA network (Fig. 3B). Curiously, none of the miRNAs are predicted to target *JUN* while *FOSB, FOS* and *ATF3* were candidates for several miRNAs. We examined expression of five miRNAs in normal and BAV aortic tissue: *mir-27a-3p, miR-144, miR-181a-5p,* and *miR-199a-5*p which are part of the network depicted in Fig. 3B. *miR-451a* was included in the analysis as it shares the same locus as *miR-144* [26]. Both *miR-27a-3p* and *miR-199a-5p* are downregulated in BAV aortic tissue while both *miR-144* and *miR-451a* are upregulated in distal aortic tissue (Fig. 3C). *miR-181a-5p* expression was not significantly different between groups.

As described, the mRNA/miRNA array analysis was done on the same set of paired tissue samples. We used the relative expression of select genes and miRNAs to determine whether paired mRNA/miRNA expression exhibited any correlation. *FOS* positively correlated with predicted target, *miR-144*, but negatively correlated with predicted target *miR-149-5p* expression (Fig. 4D). *ATF3* and *FOS* also negatively correlated with *miR-135a-5p* and *miR-199a-3p* expression, suggesting that increased miRNA expression may influence target mRNA expression in BAV tissues. To further understand why some miRNAs/mRNAs pairs expression exhibit positive correlations, we examined whether the pairs had shared predicted transcriptional regulation. Examination of predicted AP-1 miRNA regulation revealed that eight out of twenty-seven miRNA in our analysis were predicted to be ATF3, FOS or JUN target genes (Fig. 3E). Notably, *miR-149-5p* and *miR-144* were both predicted to be regulated by AP-1 transcription factors, which may explain why these miRNAs correlated with FOS expression.

3.5. A mouse model of aortic dilatation shows changes in AP-1 and miRNA gene expression similar to BAV aneurysmal tissue

AP-1 is highly responsive to stress signals, including shear stress in endothelial cells [27,28]. Aortic stenosis is one of the valve complications that is frequently seen in BAV. From our patient pool, 10 out of 15 BAV patients were classified as stenotic (Supplementary Table 1). Additionally, AP-1 and *miR-27a-3p*, *miR-144* and *miR-451a* expression loosely correlated to patterns of aortic valve area and aortic valve peak gradient (Supplementary Fig. S6). To determine how changes in aortic hemodynamic stress could affect changes in AP-1 expression, and to understand the progressive changes in AP-1 related gene expression during aortic dilatation, we utilized a mouse model of ascending aortic constriction (Fig. 4A). Using this model, we observed a progressive increase in aortic diameter up to 4 weeks post-constriction (Fig. 4B) and histological sections showed elastin breaks, characteristic of aortic remodelling (Supplementary Fig. S7A). Changes in hemodynamic stress such as maximum aortic flow velocity and maximum aortic pressure gradient early after the constriction were consistent with elevated patterns observed in BAV (Figure Supplementary Fig. S7B, C).

We performed a time course analysis of gene expression at 3 days, or 4 weeks post-constriction to capture gene expression changes during aortic remodelling (Fig. 4C). *Mmp2* and *Mmp9* expression exhibited a time dependent change in expression and were significantly increased at 4 weeks. This trend was preceded by downregulation of *Timp1* at 3 days post-constriction while *Tgf-β1*, a potential mediator of aortic dilatation in BAV, was increased. Examination of AP-1 factors revealed that *Jun* was significantly downregulated at all stages compared to Sham control (Fig. 4C). *Fos* expression was not significantly affected. Interestingly when we looked at miRNAs identified as part of our AP-1 regulatory network, we observed downregulation of *miR-27a-3p* at all timepoints while *miR-144, miR-181a-5p*, and *miR-199a-5p* were upregulated at either 3 days or 4 weeks post-constriction (Fig. 4D). This shows that gene patterns observed in BAV aortic tissue are also dysregulated during progressive dilatation in a model of aortic constriction.

3.6. AP-1/FOS inhibition leads to changes in predicted target mRNA and miRNA

To determine whether AP-1 may be regulating expression of the mRNAs or miRNAs identified in our network we cultured BAV SMCs and treated them with an AP-1 inhibitor (SR-11032) or transfected them with an siRNA targeting FOS. First BAV SMCs were characterized for FOS activity. We observed that total FOS and phosphorylated FOS at Threonine 325, an ERK1/2-dependent modification that promotes transcriptional activity, were enriched in the nucleus. We also observed expression of MMP-2 in cultured BAV SMCs. *MMP-2* and *MMP-9* are predicted AP-1 target genes in other models of aortic aneurysm [29]. SR-11032 treatment reduced *MMP-2* and *MMP-9* in paired patient samples. Three additional genes (*TIMP-1, CCN1 and CCN2*) were assessed but expression was unaffected by AP-1 inhibition (Supplementary Fig. S8). *miR-27a-3p*, *miR-181a-5p* and *miR-199a-5p* expression was also unchanged. Unfortunately, we did not detect *miR-144* in cultured BAV SMCs, as the CT expression values were above detection levels.

Using siRNA we selectively inhibited FOS activity (Fig. 5C). This strategy was not as robust as SR-11032 at targeting *MMP-2* and *MMP-9* expression. *TIMP-1, CCN1 and CCN2* remained unchanged by FOS knockdown (Supplementary Fig. S8). Interestingly, FOS knockdown upregulated *miR-27a-3p* expression, while *miR-181a-5p* and *miR-199a-5p* were unchanged. This indicates FOS may act as a negative regulator of *miR-27a-3p* in BAV SMCs.

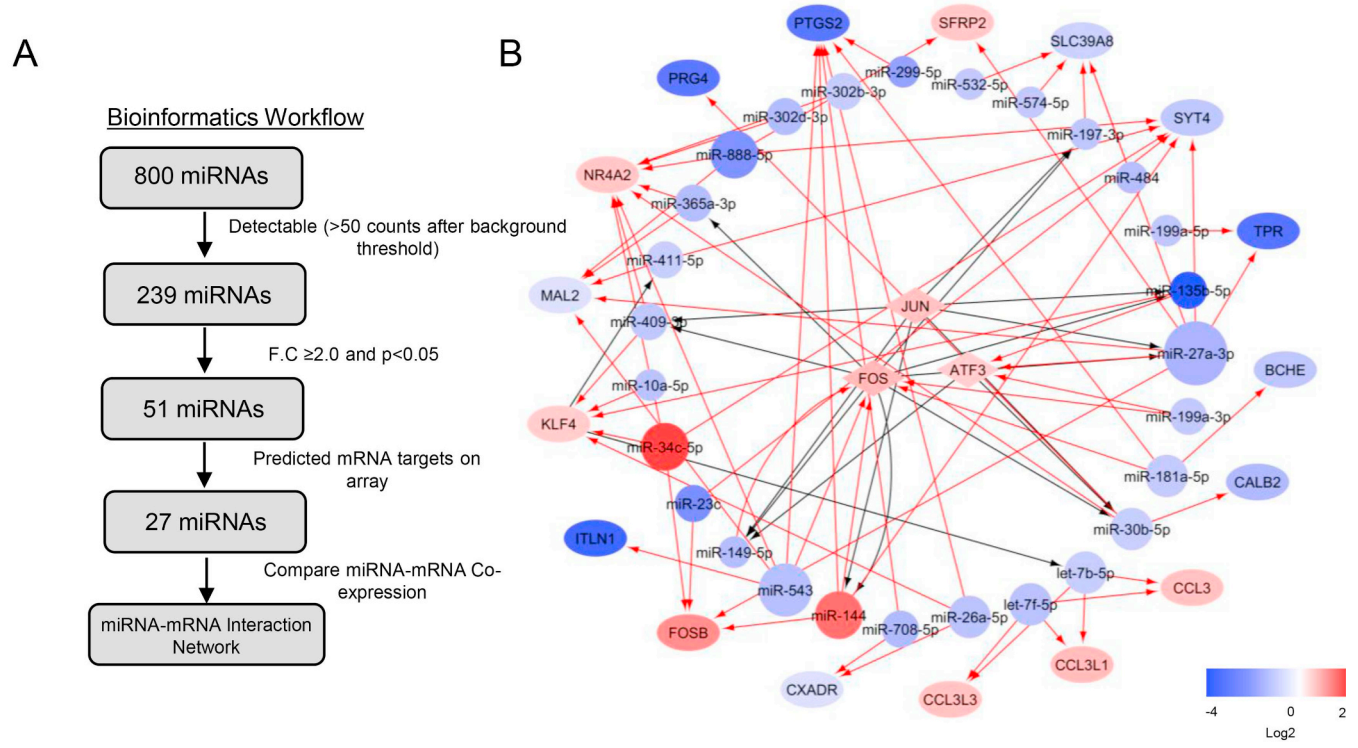

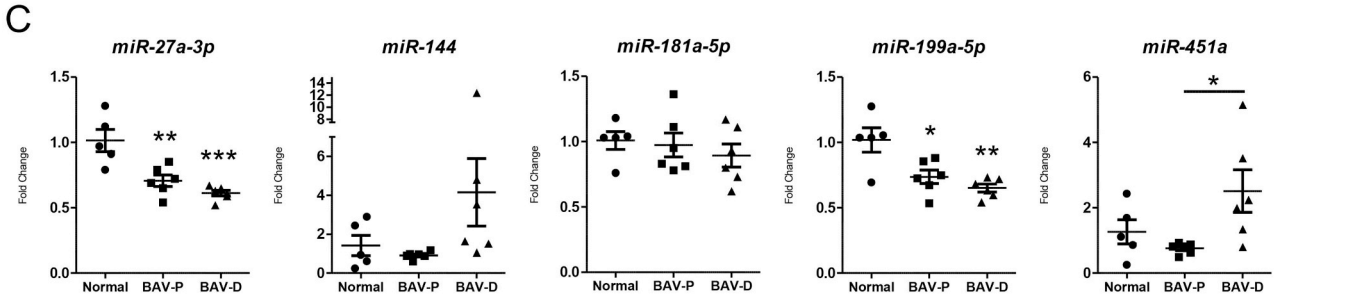

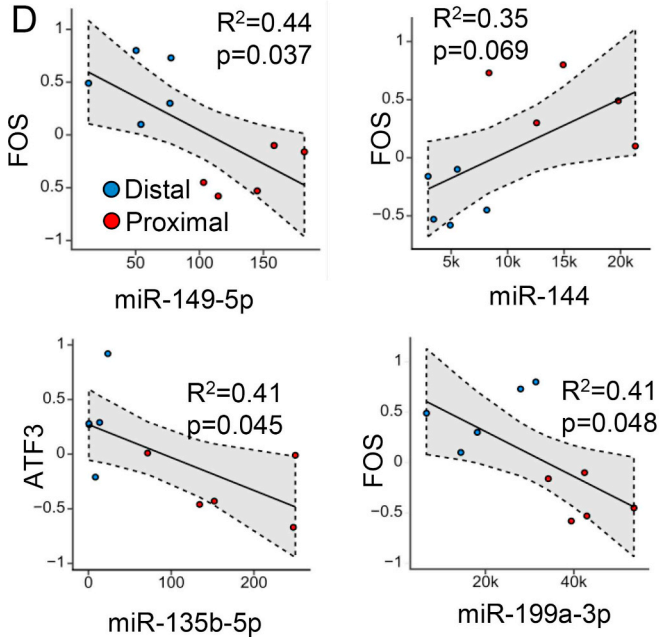

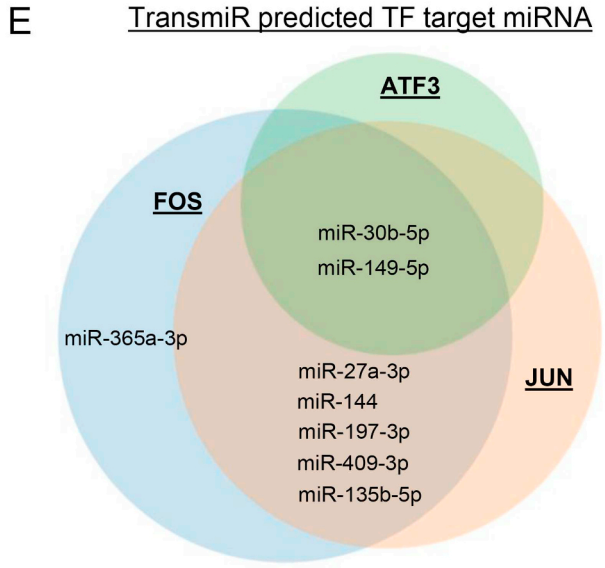

(caption on next page)

Fig. 3. AP-1 is at the centre of a microRNA regulatory network.
A) Bioinformatics workflow of significantly differentially expressed miRNA from proximal and distal BAV aortic tissue (n = 5). Paired miRNA-mRNA expression values were used to generate a miRNA-mRNA network (B). Predicted transcriptional targets are depicted using black arrows while predicted miRNA targets are depicted using red arrows. The colour of each node represents log2 expression of the gene in the distal aorta relative to the proximal aorta. Upregulated genes are red, while down regulated genes are blue. The size of each node represents the number of mRNA targets in the network. C) Validation of miRNA expression normal aorta (n = 5) compared to proximal and distal BAV aneurysmal aorta (n = 6). miRNA expression was normalized to *miR-103a-3p* expression and data are presented as fold change. *p < .05, **p < .01 and ***p < .001. D) Paired mRNA-miRNA expression datasets. Array normalized expression values from mRNA or miRNA normalized Nanostring counts were assessed for using linear regression. Blue or red dots represent distal or proximal samples, respectively. Grey area represents 95% confidence intervals. E) TransmiR predicted TF target miRNA. Eight out of twenty-seven miRNA identified from 3A are predicted transcriptional targets of FOS, JUN and ATF-3. (For interpretation of the references to colour in this figure legend, the reader is referred to the web version of this article.)

4. Discussion

Using microarray analysis of paired BAV aneurysmal tissue we found differential expression of inflammatory and endothelial gene programs, such as transcription factor family AP-1, in the distal and proximal regions of the ascending aorta. This is unique to BAV tissue as changes in AP-1 expression are not found in paired Marfan aneurysmal samples. Surprisingly, ERK1/2 activity is reduced in BAV aortic tissue, suggesting that FOS is uncoupled from the MAPK pathway. As ERK1/2 activity is restored when BAV SMCs are cultured in vitro, this may be an environmental factor such as aortic stretch. Using paired mRNA-miRNA patient samples we found that AP-1 is a central regulator and target of miRNAs in BAV aortic tissue and that these target miRNAs are differentially expressed between distal and proximal regions. Interestingly, a number of these miRNAs are stretch-responsive miRNAs (such as *miR-27a-3p* [30], and *miR-144/451a* [31]) which may be responding to changes in hemodynamics in BAV patients. Further investigation into these gene signatures using a mouse model of aortic constriction revealed time-dependent changes in AP-1, *Mmp2/9*, *Timp1*, *Tgfβ1* and miRNA expression, supporting that these changes occur with aortic remodelling. Examination of underlying transcriptional regulation showed that FOS knockdown in BAV SMCs increased the expression of *miR-27a-3p,* a miRNA downregulated in BAV aneurysmal tissue.

Our mRNA array data are consistent with other studies which show a strong correlation between BAV aortic dilatation and inflammation. Targeting inflammation is one strategy to slow aortic remodelling. Interestingly, SMC-specific deletion of Smad4 leads to increased IL-1β and aortic dilatation, but this can be reduced if treated with an IL-1β antibody [32]. Changes in the populations of immune cells during aneurysm development may also contribute to remodelling. The cell type recruited to the aortic wall is likely important as Balistreri et al. determined that BAV patients have fewer T and B cells and fewer endothelial progenitor cells compared to TAV patients, but the potential consequences from these observations are unknown [33,34].

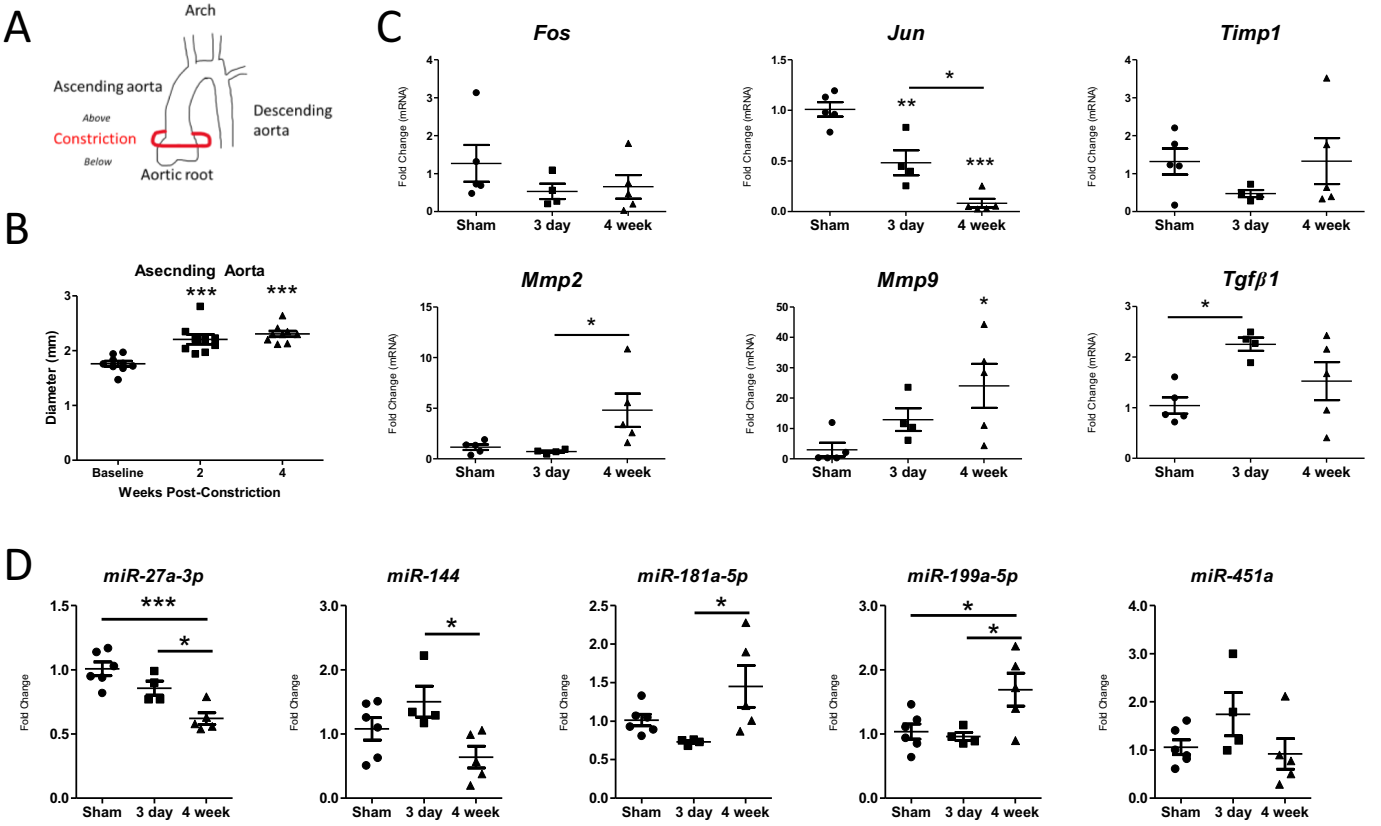

Fig. 4. A mouse model of aortic constriction recapitulates aortic dilatation and gene expression patterns observed in BAV.
A) Cartoon depicting location of the constriction site of the mouse ascending aorta. B) Ascending aortic diameter increased 2 and 4 weeks after aortic constriction in mice (n = 9) C) Time course of differential gene expression at 3 days (n = 4) or 4 weeks post-aortic constriction (n = 5) compared to 4 week Sham (n = 5). Data were normalized to *Gapdh*. D) Expression of miRNA associated with AP-1 regulation during mouse aortic constriction. miRNA expression was assessed at three days (n = 4) or 4 weeks post-aortic constriction (n = 5) compared to 4 week Sham (n = 6) and normalized to *miR-103a-3p*. All data were analyzed using a one-way ANOVA. *p < .05, **p < .01 and ***p < .001.

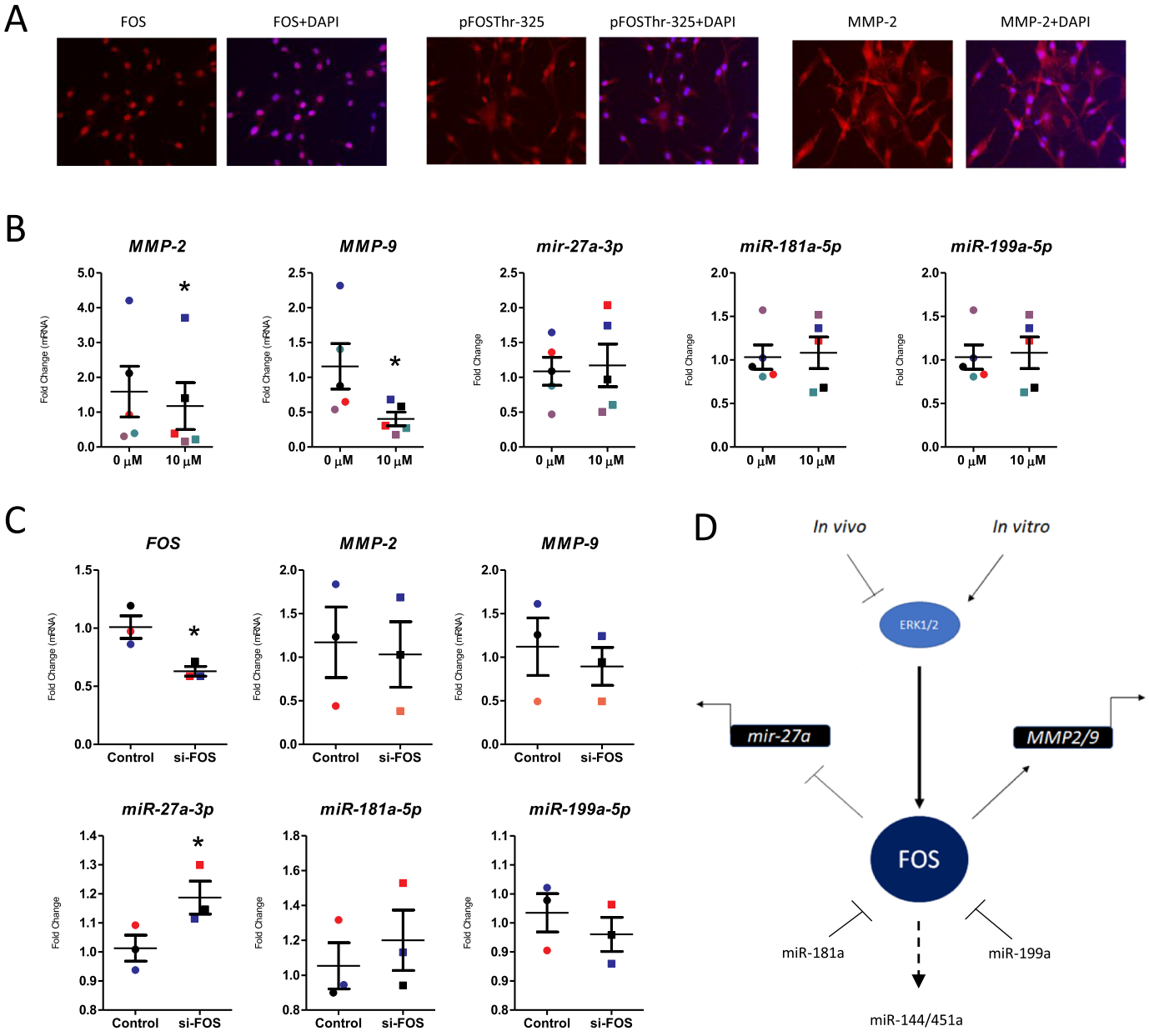

Fig. 5. FOS knockdown affects expression of *mir-27a-3p*, a stretch responsive microRNA.
A) Cultured BAV SMCs express nuclear total FOS and p-FOSThr325 and ubiquitous MMP-2. B) The effect of AP-1 inhibitor, SR-11302, on putative AP-1 target genes in BAV SMCs (n = 5). SR-11302 was added to normal culture medium (10 μM) for 24 h. Gene expression was analyzed by RT-qPCR. mRNA was normalized to *Gapdh* and miRNA was normalized to *miR-103a.* The colour of each dot represents cells from the same BAV patient. Paired patient samples were analyzed using a paired t-test (*$p < .05$). C) siRNA targeting *FOS* or a scrambled siRNA control were transfected into BAV SMCs at 50 nM. After 48 h, RNA was collected for gene expression analysis. Data were analyzed as described above. D) Summary of FOS and ERK1/2 involvement in BAV aortic dilatation. Based on our data, ERK1/2 activity is dependent on environmental cues that differ significantly from BAV aortic tissue and cultured BAV aortic smooth muscle cells. In cultured SMCs, ERK1/2 is active and this coincides with p-FOSThr325 expression, leading to changes in *MMP2/9* and *miR-27a-3p* expression. FOS may also interact with other miRNA as a translational target or regulator of miRNA expression.

Interestingly, we find though analysis of publicly deposited data that some of the inflammation gene signatures observed in our study may be derived from cellular responses to stretch. Indeed, the distal region which showed higher expression of inflammation related genes but had lower immune cell infiltration compared to the proximal region. Therefore it will be important in future studies to assess the relative contribution of changes in hemodynamics vs. immune cell activation in the progression of aortic dilatation.

In addition to changes in regional cellularity, we also observed regional differences in the mRNA expression of AP-1 factors JUN, FOS, FOSB, and ATF3. AP-1 has diverse roles including regulating of proliferation, inflammation and extracellular matrix remodelling (TIMP and MMP expression) [35,36] and therefore may affect aortic remodelling through multiple mechanisms. Consistent with a role of AP-1 in mediating aortic remodelling, therapeutic strategies which reduce AP-1 activity have been shown to be beneficial in the treatment of other aortic diseases. In abdominal aortic aneurysm, Yoshimura et al. showed that inhibition of JNK could reverse aortic aneurysm size in mice and this corresponded with reduced Jun activity [37]. Moreover, AP-1 decoy deoxy-oligonucleotides successfully reduced elastolysis and

inflammation in Marfan mice [29]. Here we show that ERK1/2 phosphorylation is drastically reduced in BAV aortic tissue compared to normal aortic tissue. This is surprising as high FOS protein levels generally correlate with p-ERK1/2. This pathway uncoupling indicates FOS protein levels are maintained by an unknown mechanism with three downstream possibilities in aortic tissue: 1) FOS is transcriptionally inactive, and functions as a repressor. 2) FOS is transcriptionally active despite low ERK1/2 activity. 3) FOS does not bind DNA nor contribute to gene repression or activation. Investigation into the post-translational stability of FOS may help to understand its role in disease. The regulation of NF-κB and MAPKs, JNK and p38, on FOS and other AP-1 subunits may be of particular relevance given the role of these factors in inflammation [38–40].

It is thought that a combination of genetics and wall shear stress in the ascending aorta contribute to aortic dilatation in patients with BAV. While the developmental formation of BAV has been linked to various mutations including Notch1 [41,42], a genetic cause of aortic aneurysm in BAV patients has not been clearly identified. Similarly, while it is reasonable to presume that the increased shear stress observed in the ascending aorta of BAV patients has a consequence on the ascending aorta [3], not all patients with BAV develop an aortic aneurysm and a definitive link has not been documented. Here, our analysis of mRNA and miRNA expression in BAV aortic tissue support a role of hemodynamic changes in regulating aortic tissue gene expression profiles. Consistent with this notion, previous studies have shown that ERK1/2 activity and AP-1 expression are altered in the endothelium by shear stress in vitro [27,43]. Immunostaining for FOS showed it is enriched in smooth muscle cells near the endothelial and adventitia, the former of which may represent a response to environmental stress from the lumen. Moreover, a number of our mRNA and miRNA expression changes identified have also been previously shown to be stretch-responsive (Supplementary Fig. S5). Further investigation of AP-1 in BAV is experimentally difficult, as mouse models of BAV require haploinsufficiency or show incomplete penetrance [44]. Therefore to assess a role of increased hemodynamic stress in regulating aortic remodelling we used a mouse model of aortic constriction to follow molecular changes associated with aortic remodelling. We observed marked downregulation of *Jun* and *miR-27a-3p* expression which coincided with upregulation of *Tgfβ1, Mmp2/9, miR-144, miR-181a-5p,* and *mirR-199a-5p,* suggesting that some of the molecular observations from BAV aortic tissue is driven by changes in aortic hemodynamics. Interestingly, a number of these miRNAs have been previously shown to play a role in smooth muscle function and aortic remodelling. For example, *miR-27a* is induced by AngII expression and can regulate smooth muscle proliferation and migration [45]. Moreover, smooth muscles secrete *miR-27a* in response to stretch to regulate endothelial cell activity [30]. Further investigation into the role of miRNAs in regulation in BAV aortic dilatation is needed.

The main thrust of aortic dilatation research at the molecular level has been on the role of TGF-β as this pathway has a role in diverse diseases of the connective tissue such as the Marfan and Loeys-Dietz syndromes [5,46–48]. ERK1/2 and JNK activity are upregulated in Marfan mice and this can be reversed using TGF-β, ERK1/2 and JNK antagonists [48,49], however, those antagonists failed to prevent aortic dilatation in the initial clinical trials [50]. Whether TGF-β has a causative role in aneurysm progression in BAV is complex. Guzzardi et al. identified a correlation between the expression of TGF-β in the aortic wall of BAV patients and wall shear stress [6]. Alternatively, extracellular TGF-β and activation of the canonical Smad signaling pathway was reported to be reduced in BAV aneurysmal smooth muscle (Paloschi et al. 2015). These divergent findings could reflect different in cellular composition (whole tissue vs SMCs) or cultured SMCs may behave differently in vitro. Based on ERK1/2 expression in cultured SMCs from BAV patients compared to whole tissue lysates, careful interpretation of these findings is critical.

5. Limitations

One limitation of our study is the lack of understanding of FOS and AP-1 transcriptional activity in BAV aortic tissue. Characterization of genome-wide DNA-binding events would clarify the role of FOS in BAV. In addition, as FOS acts as a heterodimer with JUN family members, elucidation of the protein interactions between JUN and other transcriptional regulators would lead to a better appreciation of the role of AP-1 in aortic dilatation. Minor changes in AP-1 target gene expression by FOS knockdown may indicate compensation by other AP-1 subunits. Furthermore, as this was largely a bioinformatic interpretation of systemic mRNA/miRNA targets, further validation is needed before we can conclude these miRNAs/mRNAs contribute to aortic remodelling.

6. Conclusion

Together these data show that AP-1 and the ERK1/2 signaling pathway is involved in an miRNA network that may contribute to aortic dilatation and inflammation in BAV. Considering the role of AP-1 in other aortic diseases, these preliminary data show that further investigation of AP-1 inhibition in BAV aneurysm formation is needed and should be considered in future research into the treatment of BAV aortic aneurysm progression.

Acknowledgements

None.

Sources of funding

This work was supported by a grant from the Canadian Institutes of Health Research [332652 to R-K.L.]. R-K.L. holds a Tier 1 Canada Research Chair in Cardiac Regeneration. S.W.T. is a recipient of a Ted Rogers Centre for Heart Research Fellowship. F.J.A. is a recipient of a Canadian Institutes of Health Research Post-Doctoral Fellowship. A.Y is a recipient of a Toronto General Hospital Research Institute Fellowship.

Conflict of interest

The authors report no commercial or proprietary interest in any product or concept discussed in this article.

Appendix A. Supplementary data

Supplementary data to this article can be found online at https://doi.org/10.1016/j.yjmcc.2019.04.022.

References

[1] J.Z. Goldfinger, J.L. Halperin, M.L. Marin, A.S. Stewart, K.A. Eagle, V. Fuster, Thoracic aortic aneurysm and dissection, J. Am. Coll. Cardiol. 64 (2014) 1725–1739, https://doi.org/10.1016/j.jacc.2014.08.025.
[2] J.B. Kim, M. Spotnitz, M.E. Lindsay, T.E. MacGillivray, E.M. Isselbacher, T.M. Sundt, Risk of aortic dissection in the moderately dilated ascending aorta, J. Am. Coll. Cardiol. 68 (2016) 1209–1219, https://doi.org/10.1016/j.jacc.2016.06.025.
[3] P.W.M. Fedak, A.J. Barker, S. Verma, Year in review: bicuspid aortopathy, Curr. Opin. Cardiol. 31 (2016) 132–138, https://doi.org/10.1097/HCO.0000000000000258.
[4] J. Wu, H.-F. Song, S.-H. Li, J. Guo, K. Tsang, L. Tumiati, J. Butany, T.M. Yau, M. Ouzounian, S. Fu, T.E. David, R.D. Weisel, R.-K. Li, Progressive aortic dilation is regulated by miR-17–associated miRNAs, J. Am. Coll. Cardiol. 67 (2016) 2965–2977, https://doi.org/10.1016/j.jacc.2016.04.027.
[5] E.R. Neptune, P.A. Frischmeyer, D.E. Arking, L. Myers, T.E. Bunton, B. Gayraud, F. Ramirez, L.Y. Sakai, H.C. Dietz, Dysregulation of TGF-beta activation contributes to pathogenesis in Marfan syndrome, Nat. Genet. 33 (2003) 407–411, https://doi.org/10.1038/ng1116.
[6] D.G. Guzzardi, A.J. Barker, P. van Ooij, S.C. Malaisrie, J.J. Puthumana, D.D. Belke, H.E.M. Mewhort, D.A. Svystonyuk, S. Kang, S. Verma, J. Collins, J. Carr, R.O. Bonow, M. Markl, J.D. Thomas, P.M. McCarthy, P.W.M. Fedak, Valve-related hemodynamics mediate human bicuspid aortopathy: insights from wall shear stress

mapping, J. Am. Coll. Cardiol. 66 (2015) 892–900, https://doi.org/10.1016/j.jacc.2015.06.1310.
[7] A. Forte, A. Della Corte, M. Grossi, C. Bancone, R. Provenzano, M. Finicelli, M. De Feo, L.S. De Santo, G. Nappi, M. Cotrufo, U. Galderisi, M. Cipollaro, Early cell changes and TGFβ pathway alterations in the aortopathy associated with bicuspid aortic valve stenosis, Clin. Sci. (Lond). 124 (2013) 97–108, https://doi.org/10.1042/CS20120324.
[8] N. Grewal, A.C. Gittenberger-de Groot, M.C. DeRuiter, R.J.M. Klautz, R.E. Poelmann, S. Duim, J.H.N. Lindeman, W.M.C. Koenraadt, M.R.M. Jongbloed, S.A. Mohamed, H.-H. Sievers, A.J.J.C. Bogers, M.-J. Goumans, Bicuspid aortic valve: phosphorylation of c-kit and downstream targets are prognostic for future aortopathy, Eur. J. Cardiothorac. Surg. 46 (2014) 831–839, https://doi.org/10.1093/ejcts/ezu319.
[9] V. Paloschi, J.R. Gådin, S. Khan, H.M. Björck, L. Du, S. Maleki, J. Roy, J.H.M. Lindeman, S.A. Mohamed, T. Tsuda, A. Franco-Cereceda, P. Eriksson, Aneurysm development in patients with a bicuspid aortic valve is not associated with transforming growth factor-β activation, Arterioscler. Thromb. Vasc. Biol. 35 (2015) 973–980, https://doi.org/10.1161/ATVBAHA.114.304996.
[10] T. Tokar, C. Pastrello, A.E.M. Rossos, M. Abovsky, A.-C. Hauschild, M. Tsay, R. Lu, I. Jurisica, mirDIP 4.1—Integrative database of human microRNA target predictions, Nucleic Acids Res. 46 (2018) D360–D370, https://doi.org/10.1093/nar/gkx1144.
[11] Z. Tong, Q. Cui, J. Wang, Y. Zhou, TransmiR v2.0: an updated transcription factor-microRNA regulation database, Nucleic Acids Res. 47 (2019) D253–D258, https://doi.org/10.1093/nar/gky1023.
[12] R.M. Adam, S.H. Eaton, C. Estrada, A. Nimgaonkar, S.-C. Shih, L.E.H. Smith, I.S. Kohane, D. Bägli, M.R. Freeman, Mechanical stretch is a highly selective regulator of gene expression in human bladder smooth muscle cells, Physiol. Genomics 20 (2004) 36–44, https://doi.org/10.1152/physiolgenomics.00181.2004.
[13] K. Balachandran, M.A. Bakay, J.M. Connolly, X. Zhang, A.P. Yoganathan, R.J. Levy, Aortic valve cyclic stretch causes increased remodeling activity and enhanced serotonin receptor responsiveness, Ann. Thorac. Surg. 92 (2011) 147–153, https://doi.org/10.1016/j.athoracsur.2011.03.084.
[14] V. Patel, K. Carrion, A. Hollands, A. Hinton, T. Gallegos, J. Dyo, R. Sasik, E. Leire, G. Hardiman, S.A. Mohamed, S. Nigam, C.C. King, V. Nizet, V. Nigam, The stretch responsive microRNA miR-148a-3p is a novel repressor of *IKBKB,* NF- κ B signaling, and inflammatory gene expression in human aortic valve cells, FASEB J. 29 (2015) 1859–1868, https://doi.org/10.1096/fj.14-257808.
[15] D. Merico, R. Isserlin, O. Stueker, A. Emili, G.D. Bader, Enrichment map: a network-based method for gene-set enrichment visualization and interpretation, PLoS One 5 (2010) e13984, , https://doi.org/10.1371/journal.pone.0013984.
[16] A. Subramanian, P. Tamayo, V.K. Mootha, S. Mukherjee, B.L. Ebert, M.A. Gillette, A. Paulovich, S.L. Pomeroy, T.R. Golub, E.S. Lander, J.P. Mesirov, Gene set enrichment analysis: a knowledge-based approach for interpreting genome-wide expression profiles, Proc. Natl. Acad. Sci. 102 (2005) 15545–15550, https://doi.org/10.1073/pnas.0506580102.
[17] L. Zheng, M. Weng, M. Qi, T. Qi, L. Tong, X. Hou, Q. Tong, Aberrant expression of intelectin-1 in gastric cancer: its relationship with clinicopathological features and prognosis, J. Cancer Res. Clin. Oncol. 138 (2012) 163–172, https://doi.org/10.1007/s00432-011-1088-8.
[18] S.S. Kachala, A.J. Bograd, J. Villena-Vargas, K. Suzuki, E.L. Servais, K. Kadota, J. Chou, C.S. Sima, E. Vertes, V.W. Rusch, W.D. Travis, M. Sadelain, P.S. Adusumilli, Mesothelin overexpression is a marker of tumor aggressiveness and is associated with reduced recurrence-free and overall survival in early-stage lung adenocarcinoma, Clin. Cancer Res. 20 (2014) 1020–1028, https://doi.org/10.1158/1078-0432.CCR-13-1862.
[19] L. Sun, X. Qi, Q. Tan, H. Yang, X. Qi, Low serum-butyrylcholinesterase activity as a prognostic marker of mortality associates with poor cardiac function in acute myocardial infarction, Clin. Lab. 62 (2016) 1093–1099 http://www.ncbi.nlm.nih.gov/pubmed/27468571 , Accessed date: 6 June 2017.
[20] M.E. Greenberg, L.A. Greene, E.B. Ziff, Nerve growth factor and epidermal growth factor induce rapid transient changes in proto-oncogene transcription in PC12 cells, J. Biol. Chem. 260 (1985) 14101–14110 http://www.ncbi.nlm.nih.gov/pubmed/3877054 , Accessed date: 5 April 2019.
[21] L.O. Murphy, S. Smith, R.-H. Chen, D.C. Fingar, J. Blenis, Molecular interpretation of ERK signal duration by immediate early gene products, Nat. Cell Biol. 4 (2002) 556–564, https://doi.org/10.1038/ncb822.
[22] C. Li, D.A. Scott, E. Hatch, X. Tian, S.L. Mansour, Dusp6 (Mkp3) is a negative feedback regulator of FGF-stimulated ERK signaling during mouse development, Development 134 (2007) 167–176, https://doi.org/10.1242/dev.02701.
[23] M. Ekerot, M.P. Stavridis, L. Delavaine, M.P. Mitchell, C. Staples, D.M. Owens, I.D. Keenan, R.J. Dickinson, K.G. Storey, S.M. Keyse, Negative-feedback regulation of FGF signalling by DUSP6/MKP-3 is driven by ERK1/2 and mediated by Ets factor binding to a conserved site within the DUSP6/MKP-3 gene promoter, Biochem. J. 412 (2008) 287–298, https://doi.org/10.1042/BJ20071512.
[24] E. Vorkapic, E. Dugic, S. Vikingsson, J. Roy, M.I. Mäyränpää, P. Eriksson, D. Wågsäter, Imatinib treatment attenuates growth and inflammation of angiotensin II induced abdominal aortic aneurysm, Atherosclerosis 249 (2016) 101–109, https://doi.org/10.1016/j.atherosclerosis.2016.04.006.
[25] Z.-B. Zhang, C.-C. Ruan, J.-R. Lin, L. Xu, X.-H. Chen, Y.-N. Du, M.-X. Fu, L.-R. Kong, D.-L. Zhu, P.-J. Gao, Perivascular adipose tissue–derived PDGF-D contributes to aortic aneurysm formation during obesity, Diabetes 67 (2018) 1549–1560, https://doi.org/10.2337/db18-0098.
[26] Y. Altuvia, P. Landgraf, G. Lithwick, N. Elefant, S. Pfeffer, A. Aravin, M.J. Brownstein, T. Tuschl, H. Margalit, Clustering and conservation patterns of human microRNAs, Nucleic Acids Res. 33 (2005) 2697–2706, https://doi.org/10.1093/nar/gki567.
[27] H.-J. Hsieh, N.-Q. Li, J.A. Frangos, Pulsatile and steady flow induces c-fos expression in human endothelial cells, J. Cell. Physiol. 154 (1993) 143–151, https://doi.org/10.1002/jcp.1041540118.
[28] H. Jo, K. Sipos, Y.M. Go, R. Law, J. Rong, J.M. McDonald, Differential effect of shear stress on extracellular signal-regulated kinase and N-terminal Jun kinase in endothelial cells. Gi2- and Gbeta/gamma-dependent signaling pathways, J. Biol. Chem. 272 (1997) 1395–1401, https://doi.org/10.1074/JBC.272.2.1395.
[29] R. Arif, M. Zaradzki, A. Remes, P. Seppelt, R. Kunze, H. Schröder, S. Schwill, S.M. Ensminger, P.N. Robinson, M. Karck, O.J. Müller, M. Hecker, A.H. Wagner, K. Kallenbach, AP-1 oligodeoxynucleotides reduce aortic elastolysis in a murine model of Marfan syndrome, Mol. Ther. Nucleic Acids. 9 (2017) 69–79, https://doi.org/10.1016/j.omtn.2017.08.014.
[30] L. Wang, H. Bao, K.-X. Wang, P. Zhang, Q.-P. Yao, X.-H. Chen, K. Huang, Y.-X. Qi, Z.-L. Jiang, Secreted miR-27a induced by cyclic stretch modulates the proliferation of endothelial cells in hypertension via GRK6, Sci. Rep. 7 (2017) 41058, , https://doi.org/10.1038/srep41058.
[31] K.M. Turczyńska, A. Bhattachariya, J. Säll, O. Göransson, K. Swärd, P. Hellstrand, S. Albinsson, Stretch-sensitive down-regulation of the miR-144/451 cluster in vascular smooth muscle and its role in AMP-activated protein kinase signaling, PLoS One 8 (2013) e65135, , https://doi.org/10.1371/journal.pone.0065135.
[32] F. Da Ros, R. Carnevale, G. Cifelli, D. Bizzotto, M. Casaburo, M. Perrotta, L. Carnevale, I. Vinciguerra, S. Fardella, R. Iacobucci, G.M. Bressan, P. Braghetta, G. Lembo, D. Carnevale, Targeting interleukin-1β protects from aortic aneurysms induced by disrupted transforming growth factor β signaling, Immunity 47 (2017) 959–973 (e9), https://doi.org/10.1016/j.immuni.2017.10.016.
[33] C.R. Balistreri, S. Buffa, A. Allegra, C. Pisano, G. Ruvolo, G. Colonna-Romano, D. Lio, G. Mazzesi, S. Schiavon, E. Greco, S. Palmerio, S. Sciarretta, E. Cavarretta, A.G.M. Marullo, G. Frati, A typical immune T/B subset profile characterizes bicuspid aortic valve: in an old status? Oxidative Med. Cell. Longev. 2018 (2018) 1–9, https://doi.org/10.1155/2018/5879281.
[34] C.R. Balistreri, F. Crapanzano, L. Schirone, A. Allegra, C. Pisano, G. Ruvolo, M. Forte, E. Greco, E. Cavarretta, A.G.M. Marullo, S. Sciarretta, G. Frati, Deregulation of Notch1 pathway and circulating endothelial progenitor cell (EPC) number in patients with bicuspid aortic valve with and without ascending aorta aneurysm, Sci. Rep. 8 (2018) 13834, , https://doi.org/10.1038/s41598-018-32170-2.
[35] M.R. Bergman, S. Cheng, N. Honbo, L. Piacentini, J.S. Karliner, D.H. Lovett, A functional activating protein 1 (AP-1) site regulates matrix metalloproteinase 2 (MMP-2) transcription by cardiac cells through interactions with JunB-Fra1 and JunB-FosB heterodimers, Biochem. J. 369 (2003) 485–496, https://doi.org/10.1042/BJ20020707.
[36] H.-W. Zhang, X. Wang, Z.-H. Zong, X. Huo, Q. Zhang, AP-1 inhibits expression of MMP-2/9 and its effects on rat smooth muscle cells, J. Surg. Res. 157 (2009) e31–e37, https://doi.org/10.1016/j.jss.2009.02.015.
[37] K. Yoshimura, H. Aoki, Y. Ikeda, K. Fujii, N. Akiyama, A. Furutani, Y. Hoshii, N. Tanaka, R. Ricci, T. Ishihara, K. Esato, K. Hamano, M. Matsuzaki, Regression of abdominal aortic aneurysm by inhibition of c-Jun N-terminal kinase, Nat. Med. 11 (2005) 1330–1338, https://doi.org/10.1038/nm1335.
[38] S. Wesselborg, M.K. Bauer, M. Vogt, M.L. Schmitz, K. Schulze-Osthoff, Activation of transcription factor NF-kappaB and p38 mitogen-activated protein kinase is mediated by distinct and separate stress effector pathways, J. Biol. Chem. 272 (1997) 12422–12429, https://doi.org/10.1074/JBC.272.19.12422.
[39] Y.D. Jung, F. Fan, D.J. McConkey, M.E. Jean, W. Liu, N. Reinmuth, O. Stoeltzing, S.A. Ahmad, A.A. Parikh, N. Mukaida, L.M. Ellis, Role of P38 MAPK, AP-1, and NF-kappaB in interleukin-1beta-induced IL-8 expression in human vascular smooth muscle cells, Cytokine. 18 (2002) 206–213 http://www.ncbi.nlm.nih.gov/pubmed/12126643 , Accessed date: 5 April 2019.
[40] S. Fujioka, J. Niu, C. Schmidt, G.M. Sclabas, B. Peng, T. Uwagawa, Z. Li, D.B. Evans, J.L. Abbruzzese, P.J. Chiao, NF-kappaB and AP-1 connection: mechanism of NF-kappaB-dependent regulation of AP-1 activity, Mol. Cell. Biol. 24 (2004) 7806–7819, https://doi.org/10.1128/MCB.24.17.7806-7819.2004.
[41] V. Garg, A.N. Muth, J.F. Ransom, M.K. Schluterman, R. Barnes, I.N. King, P.D. Grossfeld, D. Srivastava, Mutations in NOTCH1 cause aortic valve disease, Nature 437 (2005) 270–274, https://doi.org/10.1038/nature03940.
[42] S.H. McKellar, D.J. Tester, M. Yagubyan, R. Majumdar, M.J. Ackerman, T.M. Sundt, Novel NOTCH1 mutations in patients with bicuspid aortic valve disease and thoracic aortic aneurysms, J. Thorac. Cardiovasc. Surg. 134 (2007) 290–296, https://doi.org/10.1016/j.jtcvs.2007.02.041.
[43] H. Tseng, T.E. Peterson, B.C. Berk, Fluid shear stress stimulates mitogen-activated protein kinase in endothelial cells, Circ. Res. 77 (1995).
[44] B. Giusti, E. Sticchi, R. De Cario, A. Magi, S. Nistri, G. Pepe, Genetic bases of bicuspid aortic valve: the contribution of traditional and high-throughput sequencing approaches on research and diagnosis, Front. Physiol. 8 (2017) 612, https://doi.org/10.3389/fphys.2017.00612.
[45] M.-M. Xu, H.-Y. Deng, H.-H. Li, MicroRNA-27a regulates angiotensin II-induced vascular smooth muscle cell proliferation and migration by targeting α-smooth muscle-actin in vitro, Biochem. Biophys. Res. Commun. 509 (2019) 973–977, https://doi.org/10.1016/j.bbrc.2019.01.047.
[46] B.L. Loeys, J. Chen, E.R. Neptune, D.P. Judge, M. Podowski, T. Holm, J. Meyers, C.C. Leitch, N. Katsanis, N. Sharifi, F.L. Xu, L.A. Myers, P.J. Spevak, D.E. Cameron, J. De Backer, J. Hellemans, Y. Chen, E.C. Davis, C.L. Webb, W. Kress, P. Coucke, D.B. Rifkin, A.M. De Paepe, H.C. Dietz, A syndrome of altered cardiovascular, craniofacial, neurocognitive and skeletal development caused by mutations in TGFBR1 or TGFBR2, Nat. Genet. 37 (2005) 275–281, https://doi.org/10.1038/ng1511.

[47] B.L. Loeys, U. Schwarze, T. Holm, B.L. Callewaert, G.H. Thomas, H. Pannu, J.F. De Backer, G.L. Oswald, S. Symoens, S. Manouvrier, A.E. Roberts, F. Faravelli, M.A. Greco, R.E. Pyeritz, D.M. Milewicz, P.J. Coucke, D.E. Cameron, A.C. Braverman, P.H. Byers, A.M. De Paepe, H.C. Dietz, Aneurysm syndromes caused by mutations in the TGF-β receptor, N. Engl. J. Med. 355 (2006) 788–798, https://doi.org/10.1056/NEJMoa055695.

[48] T.M. Holm, J.P. Habashi, J.J. Doyle, D. Bedja, Y. Chen, C. van Erp, M.E. Lindsay, D. Kim, F. Schoenhoff, R.D. Cohn, B.L. Loeys, C.J. Thomas, S. Patnaik, J.J. Marugan, D.P. Judge, H.C. Dietz, Noncanonical TGFβ signaling contributes to aortic aneurysm progression in Marfan syndrome mice, Science 332 (2011) 358–361, https://doi.org/10.1126/science.1192149.

[49] J.P. Habashi, J.J. Doyle, T.M. Holm, H. Aziz, F. Schoenhoff, D. Bedja, Y. Chen, A.N. Modiri, D.P. Judge, H.C. Dietz, Angiotensin II type 2 receptor signaling attenuates aortic aneurysm in mice through ERK antagonism, Science 332 (2011) 361–365, https://doi.org/10.1126/science.1192152 (80-.).

[50] R.V. Lacro, H.C. Dietz, L.A. Sleeper, A.T. Yetman, T.J. Bradley, S.D. Colan, G.D. Pearson, E.S. Selamet Tierney, J.C. Levine, A.M. Atz, D.W. Benson, A.C. Braverman, S. Chen, J. De Backer, B.D. Gelb, P.D. Grossfeld, G.L. Klein, W.W. Lai, A. Liou, B.L. Loeys, L.W. Markham, A.K. Olson, S.M. Paridon, V.L. Pemberton, M.E. Pierpont, R.E. Pyeritz, E. Radojewski, M.J. Roman, A.M. Sharkey, M.P. Stylianou, S.B. Wechsler, L.T. Young, L. Mahony, Pediatric Heart Network Investigators, Atenolol versus losartan in children and young adults with Marfan's syndrome, N. Engl. J. Med. 371 (2014) 2061–2071, https://doi.org/10.1056/NEJMoa1404731.